THE JOURNAL OF BIOLOGICAL CHEMISTRY VOL. 291, NO. 24, pp. 12514–12526, June 10, 2016

Silencing of Small Valosin-containing Protein-interacting Protein (SVIP) Reduces Very Low Density Lipoprotein (VLDL) Secretion from Rat Hepatocytes by Disrupting Its Endoplasmic Reticulum (ER)-to-Golgi Trafficking*

Received for publication, November 18, 2015, and in revised form, March 30, 2016 Published, JBC Papers in Press, April 15, 2016, DOI 10.1074/jbc.M115.705269

Samata Tiwari[1], **Shaila Siddiqi**[1], **Olga Zhelyabovska, and Shadab A. Siddiqi**[2]

From the Burnett School of Biomedical Sciences, College of Medicine, University of Central Florida, Orlando, Florida 32827

The transport of nascent very low density lipoprotein (VLDL) particles from the endoplasmic reticulum (ER) to the Golgi determines their secretion by the liver and is mediated by a specialized ER-derived vesicle, the VLDL transport vesicle (VTV). Our previous studies have shown that the formation of ER-derived VTV requires proteins in addition to coat complex II proteins. The VTV proteome revealed that a 9-kDa protein, small valosin-containing protein-interacting protein (SVIP), is uniquely present in these specialized vesicles. Our biochemical and morphological data indicate that the VTV contains SVIP. Using confocal microscopy and co-immunoprecipitation assays, we show that SVIP co-localizes with apolipoprotein B-100 (apoB100) and specifically interacts with VLDL apoB100 and coat complex II proteins. Treatment of ER membranes with myristic acid in the presence of cytosol increases SVIP recruitment to the ER in a concentration-dependent manner. Furthermore, we show that myristic acid treatment of hepatocytes increases both VTV budding and VLDL secretion. To determine the role of SVIP in VTV formation, we either blocked the SVIP protein using specific antibodies or silenced SVIP by siRNA in hepatocytes. Our results show that both blocking and silencing of SVIP lead to significant reduction in VTV formation. Additionally, we show that silencing of SVIP reduces VLDL secretion, suggesting a physiological role of SVIP in intracellular VLDL trafficking and secretion. We conclude that SVIP acts as a novel regulator of VTV formation by interacting with its cargo and coat proteins and has significant implications in VLDL secretion by hepatocytes.

Aberrant secretion of very low density lipoproteins (VLDLs) from the liver contributes to the development of dyslipidemia, which constitutes a major risk factor for various metabolic disorders. A number of environmental and genetic factors have been identified that affect VLDL secretion. Insulin resistance is one of the most studied and a common factor that increases VLDL secretion from the liver as evident by both *in vitro* and *in vivo* studies (1–3). In contrast, hepatic infection with hepatitis C virus results in reduced VLDL secretion (4–6). Although the significance of VLDL secretion and the factors affecting this process have been very well studied by numerous groups, the molecular mechanisms that control intracellular VLDL movement along the secretory pathway are poorly understood (7–9). We have adopted a proteomic, biochemical, and molecular approach to dissect the molecular machinery that controls intracellular VLDL trafficking and its eventual secretion (8, 10–12).

Several studies have shown that VLDLs are synthesized in the endoplasmic reticulum (ER)[3] and exported to the Golgi for their maturation (13, 14). The transport of nascent VLDLs from the ER to the Golgi determines the rate of their eventual secretion, and this step is mediated by a dedicated vesicular system that utilizes a unique vesicle, the VLDL transport vesicle (VTV), which buds off the hepatic ER (7–9). Nascent VLDL particles are selectively packaged into the VTVs that specifically travel to and fuse with the Golgi and deliver VLDL particles to the Golgi lumen (8, 12). These VLDL-containing vesicles have been shown to be different from other ER-derived secretory protein transport vesicles in size, density, and protein composition; however, both transport carriers require coat complex II (COPII) for their formation from the ER (7–9). The COPII coat is composed of five different cytosolic proteins, Sar1, Sec23-Sec24, and Sec13-Sec31, which are recruited on the ER surface in an ordered manner, leading to cargo selection and vesicle formation (15–17). Emerging evidence, stemming from a number of studies carried out at the molecular level, suggests that the formation of different types of vesicles from the ER requires proteins in addition to COPII components (11, 18–24). These additional proteins provide cargo selectivity and flexibility to build a larger COPII cage that can accommodate oversized cargoes (11, 19, 21, 23).

* This work was supported by NIDDK, National Institutes of Health Grant RO1 DK-81413 (to S. A. S.). The authors have no conflict of interest to report. The content is solely the responsibility of the authors and does not necessarily represent the official views of the National Institutes of Health.

[1] Both authors contributed equally to this work.

[2] To whom correspondence should be addressed: Burnett School of Biomedical Sciences, College of Medicine, University of Central Florida, 6900 Lake Nona Blvd., Rm. 349, Orlando, FL 32827. Tel.: 407-266-7041; Fax: 407-266-7002; E-mail: shadab.siddiqi@ucf.edu.

[3] The abbreviations used are: ER, endoplasmic reticulum; VTV, VLDL transport vesicle; COPII, coat complex II; SVIP, small VCP-interacting protein; VCP, valosin-containing protein; MA, myristic acid; ERAD, endoplasmic reticulum-associated degradation; L-FABP, liver fatty acid-binding protein; TAG, triacylglycerol; ANOVA, analysis of variance; PCTV, prechylomicron transport vesicle; KLHL12, Kelch-like 12; cideB, cell death-inducing DFF45-like effector b; siSVIP, SVIP siRNA; siControl, control siRNA; ER (siControl), ER membranes isolated from siControl hepatocytes; ER (siSVIP), ER membranes isolated from siSVIP hepatocytes.

Because the VTV carries a distinct large cargo, nascent VLDL, we expect that proteins in addition to COPII components would be involved in VTV biogenesis and VLDL packaging. We performed a detailed proteomic analysis to find proteins uniquely present in the VTV (10). The VTV proteome revealed several proteins that are not present in other ER-derived vesicles; one of these VTV-specific proteins was identified as a small VCP-interacting protein (SVIP) (10). SVIP is a small 9-kDa protein consisting of 76 amino acids that contains a myristoylation site at the N terminus and is a known adaptor protein for a multifunctional protein, VCP/p97 (25). It has been reported that myristoylation of the glycine 2 residue of SVIP facilitates its attachment to the ER membrane (25). That SVIP is an ER peripheral protein and localized to the cytosolic side of the ER membrane has been demonstrated by its degradation by proteinase K treatment (26). Interestingly, SVIP inhibits endoplasmic reticulum-associated degradation (ERAD) either by blocking the formation of a trimeric complex (composed of VCP/p97, derlin, and Grp78), which mediates ERAD, or by dissociating the trimeric complex (26). This inhibitory function of SVIP indicates its role in nascent protein transport from the ER to the Golgi. Moreover, overexpression of Grp78 leads to degradation and decreased secretion of apoB100, the core protein of VLDL (27). ApoB100 is required for structural stability of the VLDL particle and mediates its transport in plasma (28). The reduced secretion of apoB100 suggests that Grp78 negatively regulates VLDL secretion because plasma apoB100 exists in VLDL. Because SVIP blocks the interaction between Grp78 and other proteins of ERAD, it might protect apoB100 from degradation and thus facilitate VLDL secretion. However, a functional role of SVIP in ER-to-Golgi transport of nascent VLDLs and their eventual secretion from hepatocytes remains to be determined.

In this study, we attempted to explore the role of SVIP in the VTV-mediated ER exit of nascent VLDL particles and their secretion from the primary hepatocytes. We demonstrate that SVIP is concentrated in VTVs and specifically interacts with both the VTV cargo protein apoB100 and the COPII component Sar1b. Additionally, our data indicate a functional role of SVIP in the formation of the nascent VLDL-containing vesicle, VTV, from the ER membranes. Furthermore, our results suggest that silencing of SVIP using siRNA reduces the VLDL secretion from the hepatocyte.

Experimental Procedures

Reagents—[^{3}H]Oleic acid (45.5 Ci/mM) and [^{3}H]myristic acid (43.5 Ci/mM) were purchased from PerkinElmer Life Sciences. Reagents used for immunoblotting were procured from Bio-Rad. Enhanced chemiluminescence (ECL) reagents were purchased from GE Healthcare. Protease inhibitor mixture tablets were obtained from Roche Applied Science. Albumin was purchased from Sigma. Other biochemicals used were of analytical grade and were purchased from local companies. Sprague-Dawley rats, 150–200 g, were obtained from Harlan Laboratories (Indianapolis, IN). All procedures involving animals were carried out in accordance with the guidelines of the University of Central Florida's Institutional Animal Care and Use Committee and strictly following the Institutional Animal Care and Use Committee-approved protocol.

Antibodies—Rabbit polyclonal antibodies against rat SVIP were generated commercially (Alpha Diagnostic, Inc., San Antonio, TX) using two antigenic peptides (amino acids 18–35 and 46–60). Polyclonal antibodies against rat VAMP7 were raised in rabbits against amino acids 105–123 of rat VAMP7 (29). Goat polyclonal antibodies to calnexin, Ykt6, GOS28, Sec13, VCP/p97, and Sec23; rabbit polyclonal antibodies to liver fatty acid-binding protein (L-FABP); goat anti-rabbit IgG Texas Red-conjugated; and bovine anti-goat IgG fluorescein isothiocyanate-conjugated antibodies were purchased from Santa Cruz Biotechnology, Inc. (Santa Cruz, CA). Rabbit polyclonal anti-Sar1 antibodies were generated commercially and have been described previously (8). Mouse monoclonal antibodies to rBet1 were procured from Stressgen (Vancouver, Canada). Rabbit polyclonal antibody to syntaxin 5 was a gift from Dr. William Balch (Scripps Research Institute, La Jolla, CA), rabbit anti-rat albumin antibody was purchased from Bethyl Laboratories, Inc. (Montgomery, TX), and rabbit polyclonal anti-apoB antibodies were a gift from Dr. Larry Swift (Department of Pathology, Vanderbilt University, Nashville, TN). Rabbit anti-goat IgG and goat anti-rabbit IgG conjugated with agarose beads were purchased from Sigma.

Cell Culture—Primary hepatocytes were isolated from adult male Sprague-Dawley rats using exactly the same procedure as described previously (11). Rat hepatoma cells (McARH7777) were obtained from American Type Culture Collection (ATCC) and were cultured in Dulbecco's modified Eagle's medium (Life Technologies) supplemented with 10% FBS (Life Technologies) and 1% penicillin-streptomycin (Sigma Co) in 5% CO_2, and the medium was changed every alternate day.

Metabolic Labeling of Hepatocytes and Isolation of ER and Golgi—Hepatocytes were metabolically labeled using [^{3}H]oleic acid, and the ER containing [^{3}H]triacylglycerol (TAG) was prepared using the same procedure as described previously (11, 30). Briefly, freshly isolated primary hepatocytes or McARH7777 cells were washed once with buffer A (136 mM NaCl, 11.6 mM KH_2PO_4, 8 mM Na_2HPO_4, 7.5 mM KCl, 0.5 mM dithiothreitol, pH 7.2) and resuspended in buffer A supplemented with [^{3}H]oleic acid (100 μCi) complexed with bovine serum albumin (BSA) and incubated at 37 °C for 35–40 min. Postincubation, cells were washed with 2% BSA in PBS to remove excess [^{3}H]oleic acid-BSA complex. Hepatocytes were then resuspended in 0.25 M sucrose in 10 mM Hepes containing 50 mM EDTA and protease inhibitors (Roche Diagnostics GmbH) and homogenized using a Parr cell disruption vessel at 1,100 p.s.i. for 40 min followed by isolation and purification of the ER and Golgi using a sucrose step gradient as reported earlier (8, 30, 31).

Preparation of Hepatic Cytosol—Hepatic cytosol was prepared utilizing the same methodology as reported previously (8, 30). In brief, freshly harvested hepatocytes were washed once with buffer B (25 mM Hepes, 125 mM KCl, 2.5 mM $MgCl_2$, 0.5 mM DTT, protease inhibitors, pH 7.2) and homogenized using a Parr cell disruption vessel at 1,100 p.s.i. for 40 min followed by ultracentrifugation at 40,000 rpm for 95 min (Beckman rotor 70.1 Ti). The resultant supernatant (cytosol) was collected, dia-

lyzed overnight against cold buffer B at 4 °C, and then concentrated to a final concentration of ~20 mg/ml protein using a Centricon filter (Amicon, Beverly, MA) with a 10-kDa cutoff.

In Vitro VTV Formation Assay—To prepare VTVs, an *in vitro* ER budding assay that has been well established in our laboratory was performed (8). [^{3}H]TAG-containing ER (500 μg of protein), resuspended in transport buffer (30 mM Hepes, 250 mM sucrose, 2.5 mM magnesium acetate, 30 mM KCl, pH 7.2), was incubated with cytosol (1 mg of protein), an ATP-regenerating system, 5 mM Mg^{2+}, 5 mM Ca^{2+}, 5 mM DTT, 1 mM GTP, and 1 mM diethyl *p*-nitrophenyl phosphate at 37 °C for 30 min. Postincubation, the reaction mixture was layered on top of a sucrose continuous gradient (0.1–1.15 M). The gradient was resolved by centrifugation using Beckman rotor SW41 at 25,900 rpm for 2 h at 4 °C, fractions (500 μl) were collected across the gradient, and associated [^{3}H]TAG dpm were determined (8).

Preparation of Whole Cell Extract—Cells were lysed in radioimmune precipitation assay buffer (Thermo Scientific, Rockford, IL) containing protease inhibitors. The resultant cell extract was centrifuged at 13,000 × *g* for 15 min, and the supernatant was collected.

Co-immunoprecipitation, SDS-PAGE, and Immunoblotting Analysis—Samples (250 μg of protein) were solubilized in 2% Triton X-100 in PBS followed by the addition of desired primary antibodies and incubation for 4 h at 4 °C. After 4 h, appropriate secondary antibodies bound to agarose beads were added and incubated overnight at 4 °C. Immune complexes bound to agarose beads were washed seven to eight times with ice-cold PBS, and co-immunoprecipitated proteins were resolved by SDS-PAGE as described (11, 12).

For immunoblotting analysis, protein samples were separated by SDS-PAGE and transferred onto a nitrocellulose membrane (Bio-Rad). The nitrocellulose membrane was blocked with 10% (w/v) nonfat dried skimmed milk in PBS-Tween 20 followed by incubation with specific primary antibodies and appropriate secondary antibodies conjugated with HRP. Protein detection was carried out using ECL reagents and by exposing the membrane to autoradiography film (Midwest Scientific, St. Louis, MO).

Measurement of Radioactivity—Radioactivity associated with [^{3}H]TAG was determined as dpm counts utilizing the Tri-Carb 2910 TR liquid scintillation analyzer (PerkinElmer Life Sciences) (8).

Antibody Treatment of the ER—ER membranes containing [^{3}H]TAG were incubated with an equal amount of desired antibodies or preimmune IgGs for 1 h at 4 °C as described (11, 12). ER membranes were then washed with cold 0.1 M sucrose in Hepes buffer to remove unbound antibodies, resuspended in transport buffer (30 mM Hepes, 0.25 M sucrose, 2.5 mM magnesium acetate, 30 mM KCl, pH7.2), and utilized in *in vitro* assays.

Transfection with siRNA—Transfection with siRNA was carried out using the same procedure as reported before (11). Rat primary hepatocytes were transfected with SVIP siRNA, 5′-GAGUCAGACUGUAUCAUUAtt-3′ (Silencer select predesigned siRNA, Life Technologies) using a Lipofectamine delivery system according to the manufacturer's protocol (Life Technologies).

Treatment of Hepatocytes with Myristic Acid—Rat primary hepatocytes were washed with warm (37 °C) PBS and incubated with different concentrations of myristic acid-BSA complex in DMEM containing 10% FBS for 24 h. As a control, cells were treated with BSA (0.2 mM) alone in DMEM. After 24 h, cells were washed with PBS and incubated with FBS-free DMEM containing 5 μCi of BSA-bound [^{3}H]oleic acid for 2 h. Next, cells were washed two times with PBS to remove all the unbound radioactive oleic acid. At each time point, 100 μl of medium was collected in triplicates, and the radioactivity associated with [^{3}H]TAG was measured.

Determination of ApoB100 and Triglycerides Secretion—To determine apoB100 secretion, medium was collected at different time points, and apoB100 was immunoprecipitated using specific anti-apoB100 antibodies. Immunoprecipitated apoB100 was separated by SDS-PAGE and probed by immunoblotting. The amount of secreted apoB100 was determined by analyzing protein band density using the NIH ImageJ program. For triglyceride secretion, 100 μl of medium was collected in triplicates, and the radioactivity associated with [^{3}H]TAG was measured.

Statistical Analysis—Data were compared using GraphPad software (GraphPad Prism 5 software for Mac OS X version) using either a two-tailed *t* test or a one-way analysis of variance (ANOVA).

Results

SVIP Is Localized to the Hepatic ER, Cytosol, Golgi, and VTV in Primary Hepatocytes—Because VLDL is synthesized in the ER and transported first to the Golgi and then to the plasma membrane for its eventual secretion, we wished to determine the distribution of SVIP in subcellular organelles associated with its synthesis and intracellular trafficking in primary rat hepatocytes. We isolated the ER, cytosol, and Golgi from primary hepatocytes and examined their purity by immunoblotting using specific protein markers. The data presented in Fig. 1*A* demonstrate that the ER was devoid of GOS28, a marker protein for the Golgi, whereas calnexin, an ER marker protein, was present in the ER. GOS28 was enriched in Golgi, but the ER was free from GOS28. Rab11, a cytosolic protein and an endosomal/lysosomal marker protein, was not present in either the ER or Golgi (Fig. 1*A*). These results suggest that both ER and Golgi were of adequate purity and can be used for *in vitro* assays. After establishing the purity of the subcellular membranes, ER-derived VTVs were generated using an *in vitro* VTV formation assay. Immunoblotting results show that purified VTVs contain their marker proteins apoB100 and Sar1b (Fig. 1*A*). The data presented in Fig. 1*B* reveal a significant enrichment of both apoB100 and Sar1b in the VTVs, which is consistent with previous reports characterizing VLDL-containing vesicles (8, 10). We next sought to probe the presence of SVIP in VTV, ER, cytosol, and Golgi fractions using specific anti-SVIP antibodies. Based on our previous proteomic studies, we expected that SVIP would be present in VTVs and other fractions (10). Consistent with previous findings (10, 25), we observed that SVIP is present in the VTVs, ER, Golgi, and cytosol (Fig. 1*A*); however, cytosol contains significantly less SVIP than the ER, VTV, and Golgi fractions (Fig. 1*B*). Interestingly,

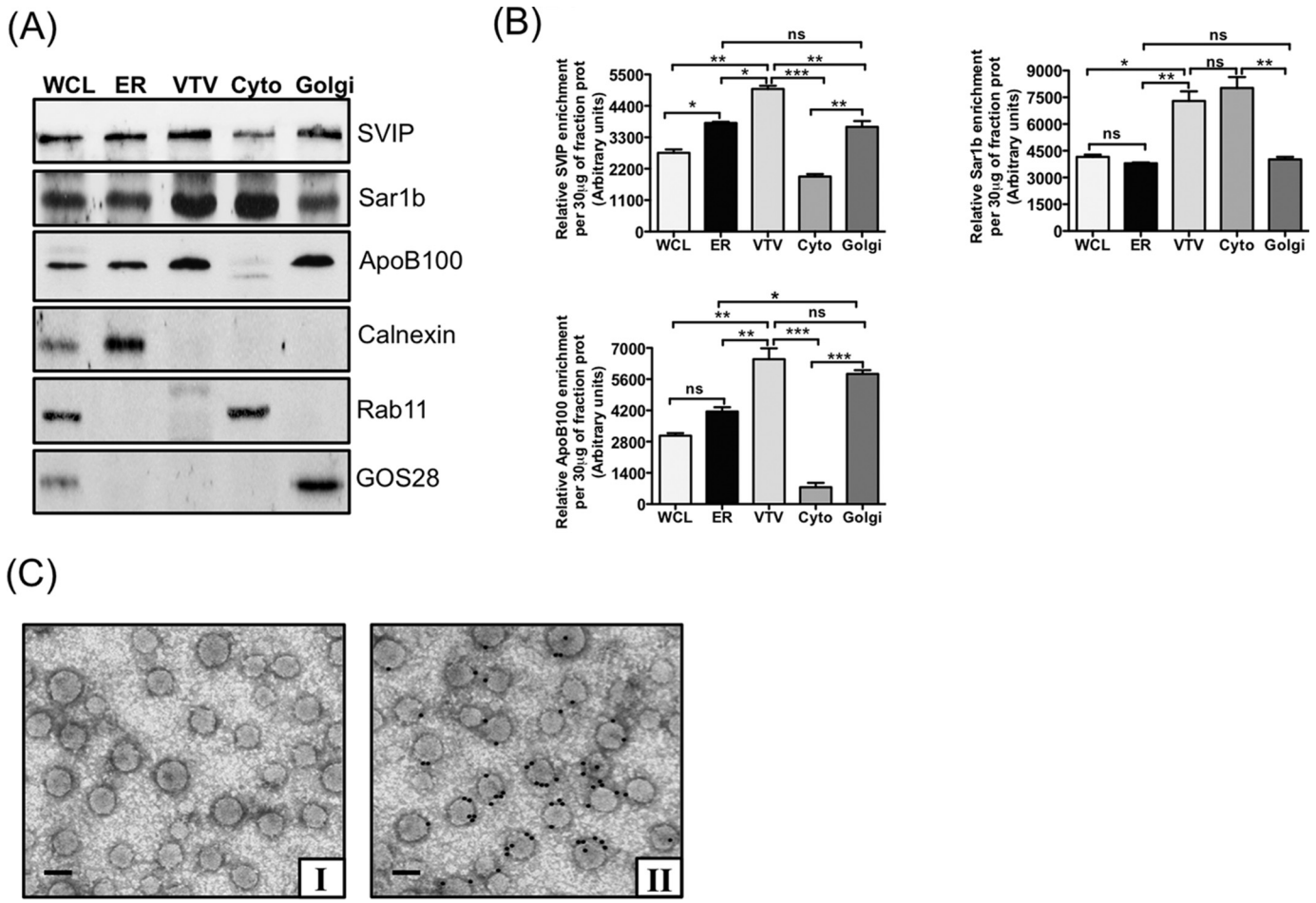

FIGURE 1. **VTV contains SVIP.** *A*, equal amounts of proteins (30 μg) from the purified fractions of ER, VTV, cytosol (*Cyto*), Golgi, and whole cell lysate (*WCL*) were separated by 12% SDS-PAGE, transblotted onto a nitrocellulose membrane, and probed with specific antibodies against the indicated proteins. ECL reagents were used to detect proteins. The data are representative of three independent experiments. *B*, the amount of SVIP, Sar1b, and apoB100 per 30 μg of fraction protein (as shown in *A*) was determined by analyzing protein band density using the NIH ImageJ program. *Error bars* represent mean ± S.D. ($n = 3$). *Bars* labeled with *asterisk* show *p* values using one-way ANOVA: *, $p < 0.05$; **, $p < 0.005$; ***, $p < 0.001$. *Bars* labeled with *ns* show non-significant *p* values. *C*, depiction of SVIP localization to the VTVs by immunoelectron microscopy. Freshly prepared VTVs were adsorbed on Formvar-carbon-coated nickel grids and incubated with either anti-rabbit preimmune IgG (*panel I*) or rabbit polyclonal anti-SVIP antibodies (*panel II*) and examined with anti-rabbit IgG conjugated with 15-nm gold particles. *Scale bars*, 100 nm.

the VTVs contain significantly more SVIP as compared with the ER membranes (Fig. 1*B*), a characteristic feature of transport vesicles, indicating that SVIP is specifically included in VTVs.

Because SVIP has not been previously reported in ER-derived vesicles, we decided to visualize the localization of SVIP to the VTVs to support our immunoblotting data with morphological evidence. To achieve this, we performed immunogold labeling of the VTV SVIP and examined the VTVs by electron microscopy using a negative staining technique as described earlier (11). Fig. 1*C* (*panel II*) clearly demonstrates that when we used anti-SVIP primary antibodies we observed strong immunogold labeling on the surface of the VTVs, indicating that SVIP is localized on the VTVs. On the contrary, no immunogold labeling was found when preimmune IgGs were used instead of anti-SVIP antibodies Fig. 1*C* (*panel I*). Together, our immunoblotting and electron microscopic data strongly suggest that the VTV contains SVIP on its surface.

Effect of Myristic Acid on ER Recruitment of SVIP—Because the N terminus of SVIP contains sites for myristoylation, which facilitates its anchorage to the ER membrane, we decided to determine the effect of myristic acid treatment on SVIP recruitment to the ER. We incubated the hepatic ER membranes with cytosol along with three different concentrations of myristic acid (0.2, 0.4, and 0.8 mM) at 4 °C for 1 h. Postincubation, the ER was separated from the reaction mixture, and the levels of SVIP recruited under varying concentrations of myristic acid were determined by immunoblotting and analyzing protein band density using NIH ImageJ. Our data presented in Fig. 2, *A* and *B*, demonstrate an increased level of ER-associated SVIP when the ER was incubated with cytosol in the presence of myristic acid as compared with control (no myristic acid). Also, we observed that incubation with myristic acid caused a steady increase in SVIP enrichment in the ER in a concentration-dependent manner (Fig. 2, *A* and *B*). Next, we wished to determine the effect of myristic acid on other proteins associated with either ER or ER-derived vesicles. Fig. 2, *A* and *B*, show that myristic acid augmented ER enrichment of Sar1b, which is required for VTV formation from hepatic ER membranes; however, there was no effect of myristic acid treatment on VCP/p97, apoB100, Sec23,

and calnexin at the ER level as shown by immunoblotting (Fig. 2*A*). Protein quantitation analyses suggest that myristic acid did not cause enrichment of VCP/p97, calnexin (Fig. 2*B*), apoB100, and Sec23 (data not shown) in the ER.

To show that the enrichment of SVIP in the ER as a result of myristic acid treatment is specific, we treated hepatic ER membranes with two different concentrations of oleic acid (0.4 and 0.8 mM) using exactly the same method. The data presented in

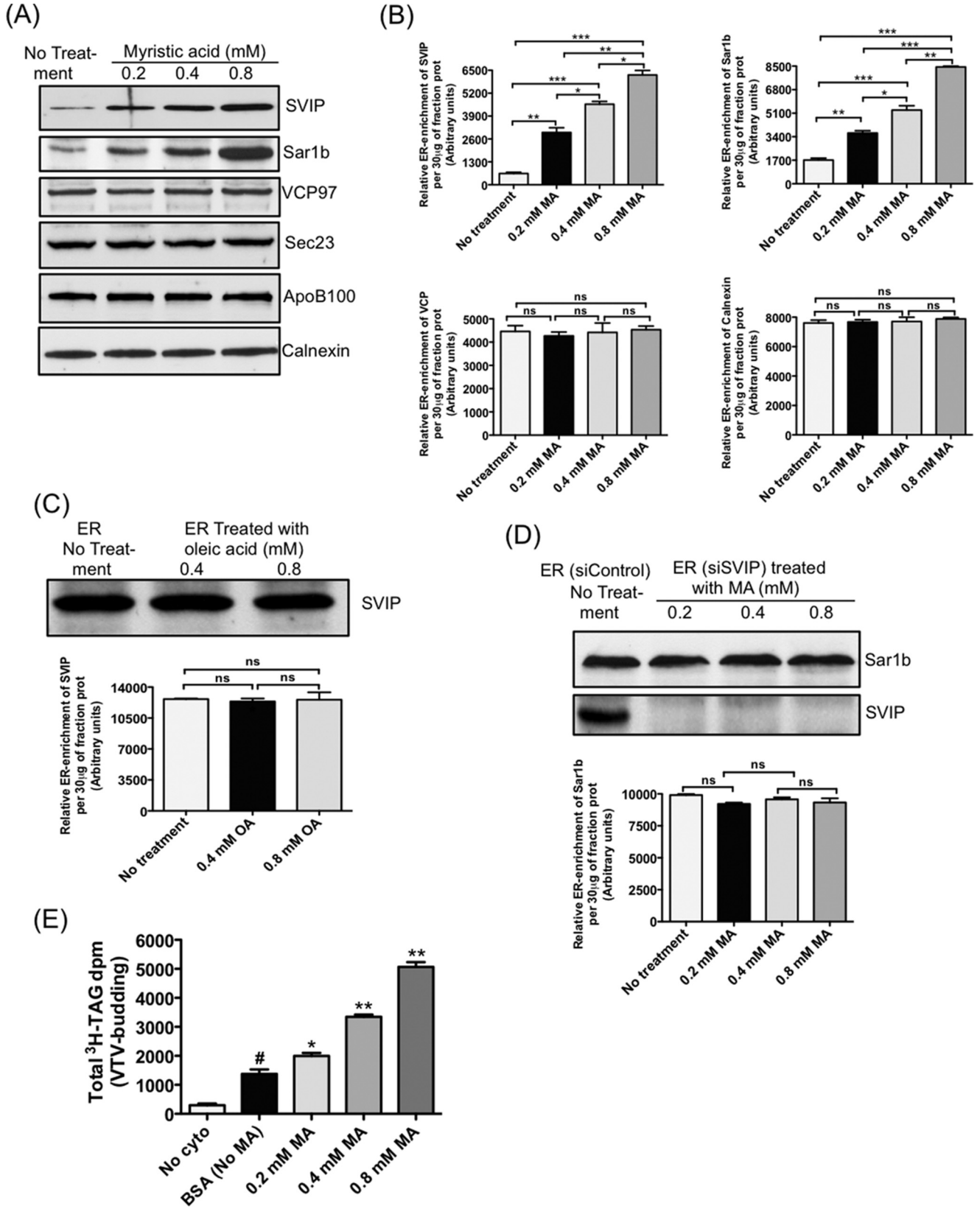

Fig. 2*C* clearly demonstrate that oleic acid treatment did not cause relative enrichment of SVIP in the ER as compared with untreated ER membranes.

Next, we wished to determine whether the increased enrichment of Sar1b in the ER after myristic acid treatment is SVIP-dependent or myristoylation of Sar1b causes its enrichment in the ER. To address this question, we knocked down the SVIP in the primary hepatocytes using siRNA (75 nM), which significantly reduced SVIP protein expression (>95%) as determined by immunoblotting analysis (data not shown); isolated the ER; and treated the ER with different concentrations of myristic acid (0.2, 0.4, and 0.8 mM) similarly as in Fig. 2*A*. Our results show that ER membranes, isolated from primary hepatocytes transfected with either control siRNA or SVIP siRNA, contain both Sar1b and SVIP (Fig. 2*D*). The ER isolated from SVIP knockdown hepatocytes did not contain SVIP (Fig. 2*D*). Interestingly, we did not see any enrichment of Sar1b in SVIP-deficient ER membranes when we treated them with increasing concentrations of myristic acid (Fig. 2*D*). These data suggest that the observed enrichment of Sar1b as a result of myristic acid treatment (as shown in Fig. 2*A*) is SVIP-dependent, and this can be further supported by our co-immunoprecipitation data indicating that SVIP interacts with Sar1b (see Fig. 5*A*).

Effect of Myristic Acid on VTV Formation—Because myristic acid treatment increased the ER recruitment of both SVIP and Sar1b, we were interested in examining its effect on VTV formation from the hepatic ER membranes. We incubated hepatocytes with myristic acid complexed with BSA at three different concentrations of myristic acid, *viz*. 0.2, 0.4, and 0.8 mM, for 72 h. After incubation, we isolated ER membranes and cytosol from myristic acid-treated hepatocytes. For control, we treated hepatocytes with BSA alone and isolated ER and cytosol. To examine the effect of myristic acid on VTV formation, we carried out an *in vitro* VTV budding assay. As shown in Fig. 2*E*, VTV formation was significantly increased when cells were treated with myristic acid as compared with BSA alone treatment. These data indicate that myristic acid increases the formation of the VTV from hepatic ER membranes.

Because myristic acid, but not oleic acid, causes a concentration-dependent increase in SVIP in the ER fraction (Fig. 2, *A* and *C*), we questioned whether or not myristoylation of SVIP is required for SVIP recruitment to the ER. In an attempt to show the role of myristoylation, we isolated the ER and cytosol from primary hepatocytes transfected with either 75 nM control (siControl) or 75 nM SVIP siRNA (siSVIP). The ER (siControl or siSVIP) was incubated under different conditions as indicated in Fig. 3*A*. After incubation, the ER membranes were separated from the reaction mixture, and SVIP recruitment to the ER under various conditions was determined by immunoblotting. As shown in Fig. 3*A*, SVIP was present in the ER that was isolated from hepatocytes transfected with control siRNA (Fig. 3*A*, *lane 1*), whereas no SVIP was found in the ER that was isolated from SVIP knockdown hepatocytes (Fig. 3*A*, *lane 2*). Interestingly, when ER membranes isolated from siSVIP hepatocytes (ER (siSVIP)) were incubated with cytosol (siSVIP), recombinant SVIP protein, enolase (20 nM), and ATP in the absence of myristic acid at 30 °C, no SVIP was found in the ER (Fig. 3*A*, *lane 3*); however, in the presence of 0.8 mM myristic acid and in the absence of enolase (an inhibitor of *N*-myristoyltransferase (38)), a strong signal of SVIP was observed in the ER (Fig. 3*A*, *lane 4*). However, when we replaced myristic acid with 0.8 mM oleic acid and included enolase to block myristoylation by inhibiting *N*-myristoyltransferase activity, we did not see any protein band for SVIP (Fig. 3*A*, *lane 5*). Under all conditions, we did not observe any change in the protein levels of calnexin, an ER-resident protein (Fig. 3*A*). Together, these data suggest that SVIP myristoylation is required for its recruitment to the ER membrane.

Next, we sought to determine the effect of SVIP myristoylation on VTV budding. We used ER membranes (siControl or siSVIP) treated under conditions as described for different lanes of Fig. 3*A* in our *in vitro* VTV budding assay. As expected, ER membranes isolated from siControl hepatocytes (ER (siControl)) gave a robust signal for VTV formation (Fig. 3*B*, *bar 1*); however, a significant increase in VTV formation was observed when ER membranes enriched in SVIP (Fig. 3*A*, *lane 4*) were used in the assay (Fig. 3*B*, *bar 4*). As demonstrated in Fig. 3*B* (*bars 2*, *3*, and *5*), VTV formation was minimal when either ER (siRNA) or ER (siRNA) incubated under conditions that do not support myristoylation were used in the budding assay. Together, our data clearly suggest that SVIP myristoylation increases its recruitment to the ER surface, leading to enhanced VTV formation from hepatic ER membranes.

FIGURE 2. **Effects of myristic acid treatment on ER enrichment of SVIP and VTV budding.** *A*, hepatic ER membranes were incubated with cytosol and different concentrations of myristic acid (0.2, 0.4, and 0.8 mM) for 1 h at 4 °C. ER membranes were separated from the reaction mixture, and protein samples (30 μg) from treated or untreated ER were assessed by immunoblotting with the indicated antibodies. *B*, the amount of SVIP Sar1b, VCP97, and calnexin per 30 μg of fraction protein (as shown in *A*) was determined by analyzing protein band density using the NIH ImageJ program. *Error bars* represent mean ± S.D. ($n = 3$). *Bars* labeled with *asterisks* show *p* values using one-way ANOVA: *, $p < 0.05$; **, $p < 0.005$; ***, $p < 0.001$. *C*, hepatic ER membranes were incubated with cytosol and different concentrations of oleic acid (*OA*) (0.4 and 0.8 mM) for 1 h at 4 °C. ER membranes were separated from the reaction mixture, and protein samples (30 μg) from treated or untreated ER were probed by immunoblotting with anti-SVIP antibodies. The amount of SVIP per 30 μg of fraction protein was determined by analyzing protein band density using the NIH ImageJ program. *Error bars* depict mean ± S.D. ($n = 3$). *Bars* labeled with *ns* show non-significant *p* values using one-way ANOVA. *D*, rat hepatocytes were transfected with a 75 nM concentration of either siSVIP or siControl (Silencer select siRNA). After transfection, ER (siControl) and ER (siSVIP) were isolated. ER (siSVIP) were incubated with cytosol and different concentrations of myristic acid (*MA*) (0.2, 0.4, and 0.8 mM) for 1 h at 4 °C. ER (siSVIP) were separated from the reaction mixture, and protein samples (30 μg) from treated ER (siSVIP) or untreated ER (siControl) were assessed by immunoblotting with either Sar1b or SVIP antibodies. The amount of Sar1b per 30 μg of fraction protein was determined by analyzing protein band density using the NIH ImageJ program. *Error bars* represent mean ± S.D. ($n = 3$). *Bars* labeled with *ns* show non-significant *p* values using one-way ANOVA. *E*, hepatocytes were incubated with myristic acid complexed with BSA at three different concentrations of myristic acid (0.2, 0.4, and 0.8 mM) for 72 h. ER containing [^{3}H]TAG and cytosol were prepared from hepatocytes that were treated with the indicated concentrations of myristic acid complexed with BSA or untreated (only BSA-treated), and VTV budding assays were performed as described under "Experimental Procedures." As a negative control, ER containing [^{3}H]TAG isolated from untreated (only BSA-treated) hepatocytes was incubated in the absence of cytosol (*No cyto*). *Error bars* depict mean ± S.D. ($n = 4$). *Bars* labeled with *asterisks* and # show *p* values compared with BSA-treated control using one-way ANOVA: *, $p < 0.05$; **, $p < 0.01$; #, $p < 0.005$ compared with negative control (absence of cytosol).

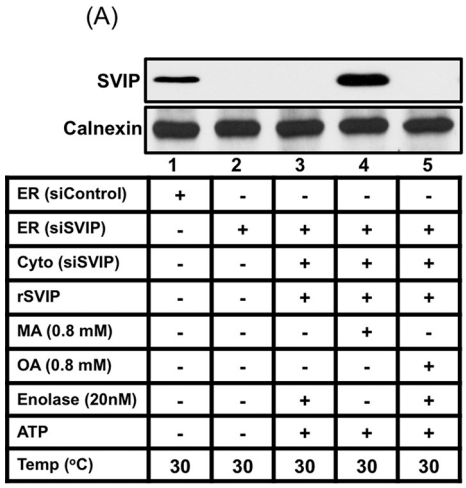

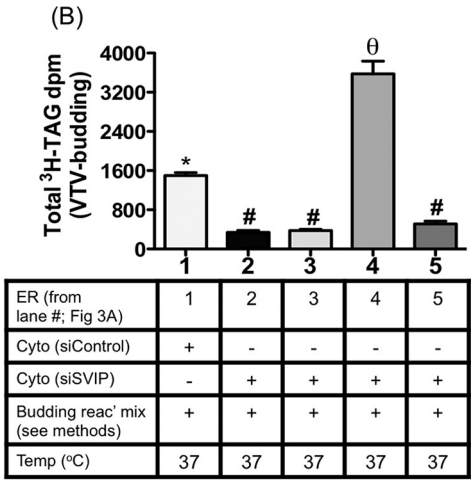

FIGURE 3. **Effects of SVIP myristoylation on recruitment of SVIP on ER membranes and VTV budding.** Rat hepatocytes were transfected with a 75 nM concentration of either siSVIP or siControl (Silencer select siRNA). After transfection, ER and cytosol were isolated from both siControl and siSVIP hepatocytes. *A*, isolated ER (siControl) and ER (siSVIP) (150 μg of protein) were incubated at 30 °C in the presence or absence of either 300 μg of cytosol (*Cyto*) siSVIP protein or 50 μg of recombinant SVIP (*rSVIP*) protein with or without myristic acid (*MA*), oleic acid (*OA*), enolase, and ATP as indicated. Postincubation, the ER membranes were separated from the reaction mixture (*reac' mix*), and protein samples (30 μg) from treated ER were probed by immunoblotting with anti-SVIP and anti-calnexin antibodies. *B*, *in vitro* VTV formation assays were carried out utilizing ER membranes containing [^{3}H]TAG and cytosol that were prepared from hepatocytes transfected with either siSVIP or siControl as indicated in the figure. Prior to performing the budding assay, ER membranes were treated as indicated in *A*. *Error bars* represent mean ± S.D. ($n = 4$). *Bars* labeled with different *symbols* show *p* values using one-way ANOVA: * *versus* #, $p < 0.002$; * *versus* θ, $p < 0.001$; θ *versus* #, $p < 0.001$; # *versus* #, *p* is non-significant.

Effect of Myristic Acid on TAG and ApoB100 Secretion—Because our data suggest that myristic acid treatment of hepatocytes induces VTV biogenesis from the ER and the ER-to-Golgi transport of VLDL is the rate-limiting step in its eventual secretion from the hepatocytes, we speculated that this would increase TAG and apoB100 secretion from the hepatocytes. To test our speculation, we treated the primary hepatocytes with 0.2, 0.4, and 0.8 mM [^{3}H]myristic acid complexed with BSA and determined the secreted [^{3}H]TAG in the medium. As expected, we observed a significant increase in TAG secretion in a concentration-dependent manner from myristic acid-treated hepatocytes as compared with control hepatocytes, which were treated with BSA alone (Fig. 4*A*). Because apoB100 is a VLDL core protein, we determined the effect of myristic acid treatment on apoB100 secreted in the medium utilizing immunoblotting followed by protein band density analysis. Our results in Fig. 4*B* show that myristic acid treatment enhanced apoB100 secretion in a concentration-dependent fashion; however, no significant change in albumin secretion was observed. Taken together, our data so far strongly suggest that myristic acid enhances SVIP recruitment on the ER surface, leading to increased VTV biogenesis and VLDL secretion from the hepatocytes.

SVIP Interacts with COPII Components—We have previously shown that the generation of VTVs from the hepatic ER requires COPII proteins and that VTVs contain SVIP (10). Moreover, our results in the current study demonstrate a significant increase in VTV formation as a result of myristic acid treatment. These observations raise the possibility that SVIP may be a part of the prebudding complex, which is required for VTV formation and thus interacts with the COPII components. This assumption is further supported by the fact that the formation of VTVs requires additional proteins that form an intricate COPII coat for the generation of larger vesicles. To determine the interaction between SVIP and COPII components, we carried out co-immunoprecipitation assays using hepatic cytosol and specific anti-SVIP antibodies and probed the same membrane separately with antibodies against each of the COPII components. Our immunoblotting results suggest that SVIP interacts with COPII proteins, Sar1, Sec23, and Sec13 as shown in Fig. 5*A*.

To substantiate our findings, we performed co-immunoprecipitation assays using cytosol and specific antibodies against Sec23 and Sec13 and examined the membrane with specific anti-SVIP antibodies. The data presented in Fig. 5*B* clearly suggest that both Sec13 and Sec23 co-immunoprecipitated SVIP from hepatic cytosol, reasserting a strong interaction between SVIP and COPII components.

SVIP Interacts with ApoB100 but Not with Albumin—Because our previous proteomic analysis has shown that SVIP is uniquely present in the VTV (10), we questioned whether SVIP interacts with the hepatic secretory protein albumin, which has been shown to be transported from the ER in protein transport vesicle and not in the VTV (8, 9). Also, we were interested in finding out whether or not SVIP interacts with VTV cargo protein apoB100 at the ER level. Consequently, we performed co-immunoprecipitation assays using solubilized hepatic ER membranes and specific anti-SVIP antibodies. After co-immunoprecipitation, protein-protein interaction was detected using immunoblotting. Our data clearly demonstrate that SVIP interacts with apoB100, but we did not observe any interaction between SVIP and albumin; however, albumin was present in the ER (Fig. 5*C*). These observations illustrate that SVIP exclusively interacts with VTV cargo protein apoB100, suggesting that SVIP may be involved in VLDL export from the hepatic ER.

To support our co-immunoprecipitation data, we decided to examine the protein-protein interaction between SVIP and

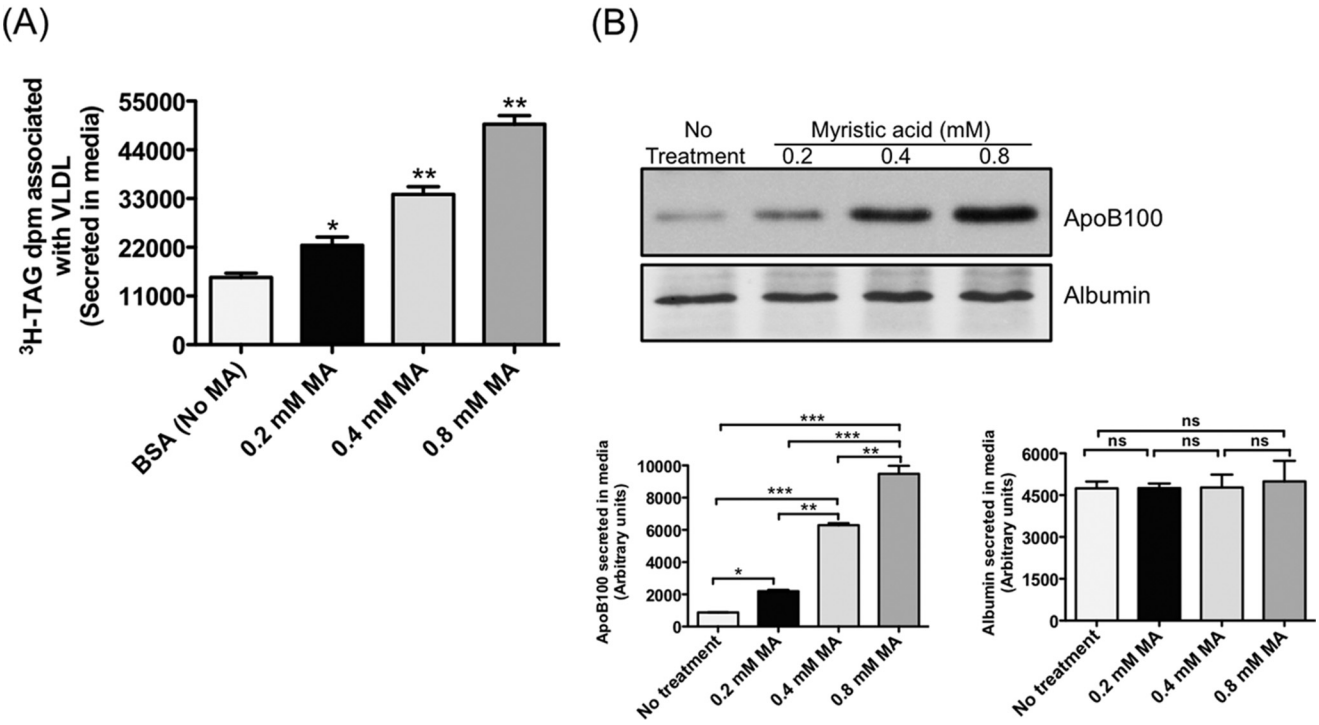

FIGURE 4. **Effects of myristic acid treatment on TAG and apoB100 secretion.** Hepatocytes were incubated with myristic acid (*MA*) complexed with BSA at three different concentrations of myristic acid (0.2, 0.4, and 0.8 mM) for 24 h. As a control, hepatocytes were treated with BSA (0.2 mM) alone in medium. Cells were washed two times with PBS to remove all the unbound radioactive myristic acid. *A*, to determine triglyceride secretion, 100 μl of medium was collected in triplicates, and the radioactivity associated with [^{3}H]TAG was measured. *Error bars* represent mean ± S.D. ($n = 4$). *Bars* labeled with *asterisks* show *p* values compared with BSA-treated control using one-way ANOVA: *, $p < 0.05$; **, $p < 0.005$. *B*, for apoB100 secretion, medium was collected, and apoB100 was immunoprecipitated using specific anti-apoB100 antibodies. Immunoprecipitated apoB100 was separated by SDS-PAGE and probed by immunoblotting. The amount of secreted apoB100 or albumin per 200 μl of medium (used for immunoprecipitation) was determined by analyzing protein band density using the NIH ImageJ program. *Error bars* depict mean ± S.D. ($n = 3$). *Bars* labeled with *asterisks* show *p* values using one-way ANOVA: *, $p < 0.05$; **, $p < 0.005$; ***, $p < 0.001$. *Bars* labeled with *ns* show non-significant *p* values.

apoB100 morphologically utilizing confocal microscopy using a double label immunofluorescence method. The data presented in Fig. 5*D* clearly suggest that SVIP co-localizes with apoB100 in reticular structures, a characteristic feature of the ER. In an attempt to determine whether the interaction between SVIP and apoB100 occurs at the ER level, we examined the localization of SVIP with an ER marker protein, calnexin. The *lower panels* of Fig. 5*D* show that SVIP indeed co-localizes with calnexin. Together, our biochemical and morphological data indicate that the protein-protein interaction between SVIP and apoB100 potentially occurs at the ER level.

Blockade of SVIP Reduces VTV Formation—Our data thus far demonstrate that SVIP is present on the VTV surface and interacts with VTV cargo protein (apoB100) and VTV coat components (Sar1, Sec 23, and Sec13) at the ER level. These observations led us to question whether or not SVIP plays any functional role in the generation of the VTV from hepatic ER. To examine the role of SVIP in VTV formation from hepatic ER, we first blocked the ER SVIP by incubating the ER membranes with either specific anti-SVIP antibodies or appropriate preimmune IgGs as a control at 4 °C for 1 h. Postincubation, unbound antibodies were removed. Because hepatic cytosol contains SVIP, we immunodepleted SVIP from the cytosol using anti-SVIP antibodies bound to agarose beads as described previously (11). As shown in Fig. 6*A*, VTV formation was significantly reduced by blocking the SVIP, whereas VTV generation continued uninterrupted when both hepatic ER membranes and cytosol were treated similarly with preimmune IgGs (Fig. 6*A*). A significant reduction in VTV formation as a result of SVIP blockade indicates that SVIP has an active role in VTV-mediated ER-to-Golgi transport of VLDL particles. To eliminate the possibility that anti-SVIP antibodies are causing steric hindrance leading to decreased VTV formation, we boiled these antibodies prior to treating the ER membranes. Our data presented in Fig. 6*A* show that the treatment of ER membranes with boiled SVIP antibodies did not affect VTV generation.

To show that the observed reduction in VTV biogenesis as a result of SVIP blocking was specific, we blocked other proteins such as rBet1, syntaxin 5, ykt6, and VAMP7, which are known to be involved in ER-to-Golgi transport, using specific antibodies and monitored the VTV budding activity. The results presented in Fig. 6*A* clearly show that VTV formation continued uninterrupted and that there was no effect of blocking each of these proteins (rBet1, syntaxin 5, ykt6, and VAMP7). These data demonstrate the specificity of reduction in VTV biogenesis as a consequence of SVIP blockade and suggest a requirement of SVIP in VLDL exit from the hepatic ER.

Because our data indicate that SVIP interacts with Sar1b, Sec13, and Sec23, it is likely that SVIP forms a prebudding complex with these proteins that triggers the process of VTV formation from the hepatic ER. To determine the role of these proteins in VTV formation, we blocked their function by immunodepleting the hepatic cytosol using specific antibodies and treating the ER membranes at 4 °C for 2 h with antibodies as

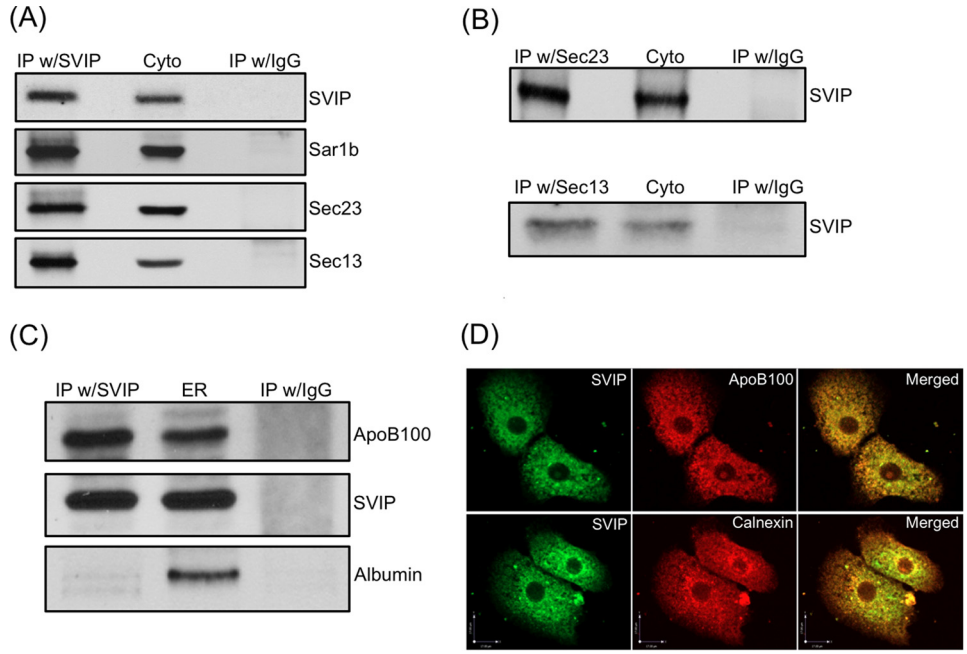

FIGURE 5. **SVIP interacts with COPII components and apoB100.** *A*, hepatic cytosol (250 μg of protein) was incubated with anti-rabbit SVIP antibody for 4 h at 4 °C followed by the addition of anti-rabbit IgGs bound to agarose beads, and incubation continued overnight at 4 °C overnight. Immune complexes bound to agarose beads were washed thoroughly with ice-cold PBS, and co-immunoprecipitated proteins were resolved by SDS-PAGE and immunoblotted against the indicated proteins. The indicated proteins were sequentially identified using a single membrane after stripping the membrane each time. ECL reagents were used for protein detection. The results are representative of four experiments. *B*, similar to *A*, antibodies against Sec23 (*upper panel*) or Sec13 (*lower panel*) were used to immunoprecipitate hepatic cytosol (250 μg of protein), and co-immunoprecipitated proteins were immunoblotted for SVIP protein. *C*, ER membranes (250 μg of protein) were solubilized in 2% (v/v) Triton X-100. Solubilized ER proteins were immunoprecipitated with anti-rabbit SVIP antibodies using exactly the same method as described in *A*. Co-immunoprecipitated proteins were separated by SDS-PAGE (8–16% gel) and immunoblotted for apoB100, SVIP, and albumin. *D*, SVIP co-localizes with apoB100 and calnexin. Rat hepatocytes were double labeled with SVIP (FITC; *green*) and apoB100 (Texas Red) (*upper panel*) and with SVIP (FITC; *green*) and calnexin (Texas Red) (*lower panel*). Merged figures demonstrate the co-localization of SVIP with apoB100 (*upper panel*) and SVIP with calnexin (*lower panel*). *IP*, immunoprecipitation; *Cyto*, cytosol. *Scale bars*, *x* axis = 17.0 μm; *y* axis = 17.0 μm.

indicated in Fig. 6*B*. Postincubation, unbound antibodies in each case were removed by washing the ER membranes. The data presented in Fig. 6*B* indicate that blocking any of Sar1b, Sec13, and Sec23 proteins results in significant reduction in the VTV formation from the ER, whereas IgG treatment did not affect VTV formation. Because our previous studies have shown that L-FABP is required for the formation of small intestinal ER-derived prechylomicron transport vesicles (PCTVs) (21), we questioned whether or not L-FABP plays a role in the formation of VTV from hepatic ER. To examine the role of L-FABP, we blocked this protein using specific antibodies and carried out a budding assay. As shown in Fig. 6*B*, VTV formation continued without any change, suggesting that L-FABP is not required for the formation of the VTV. The finding that L-FABP is not required for the biogenesis of hepatic ER-derived VTVs but is essential for the formation of intestinal ER-derived PCTVs supports our thesis that VTV formation is ATP- and GTP-dependent and requires COPII components, whereas PCTV formation does not require GTP or the COPII system (7, 8, 22, 40). However, other data[4] suggest that L-FABP is required for the formation of post-Golgi VLDL transport vesicles from hepatic *trans*-Golgi that are of the same size (~350 nm) as PCTVs (31, 40). Taken together, our data strongly suggest that SVIP interacts with COPII components (Sar1b, Sec13, and Sec23), and these proteins are required for the formation of VTV from the ER, which is consistent with previous observations (11, 12).

Silencing of SVIP Abrogates VTV Biogenesis—To clearly establish the role of SVIP in VTV formation, we decided to reduce the amount of SVIP with the relatively more robust technique of utilizing siRNA to knock down SVIP in primary hepatocytes. We used Lipofectamine as an siRNA delivery system because we have been using this approach successfully in primary hepatocytes (11). Post-transfection with either control or SVIP siRNA, the expression level of SVIP protein in hepatocytes was determined by immunoblotting. Immunoblotting data indicate that the expression of SVIP protein was significantly reduced (>90%) when cells were transfected with SVIP siRNA, whereas control siRNA did not reduce the protein expression of SVIP at all (Fig. 6*C*). However, there was no effect of SVIP siRNA on the expression of β-actin, indicating the specificity of SVIP silencing (Fig. 6*C*). After determining the SVIP knockdown in hepatocytes, we isolated the ER membranes and cytosol from these cells and probed for SVIP protein levels in the ER and cytosol. We observed that the ER isolated from SVIP siRNA (25 nM)-transfected cells contains a significantly lower amount of SVIP protein as compared with control cells, whereas when hepatocytes were transfected with either 50 or 75 nM SVIP siRNA no signal of SVIP was found in the ER (data not shown); however, the expression of an ER-resident protein, calnexin, was not affected in all cases (data not shown). Similarly, we determined that hepatic cytosol isolated from

[4] S. Siddiqi and S. A. Siddiqi, unpublished data.

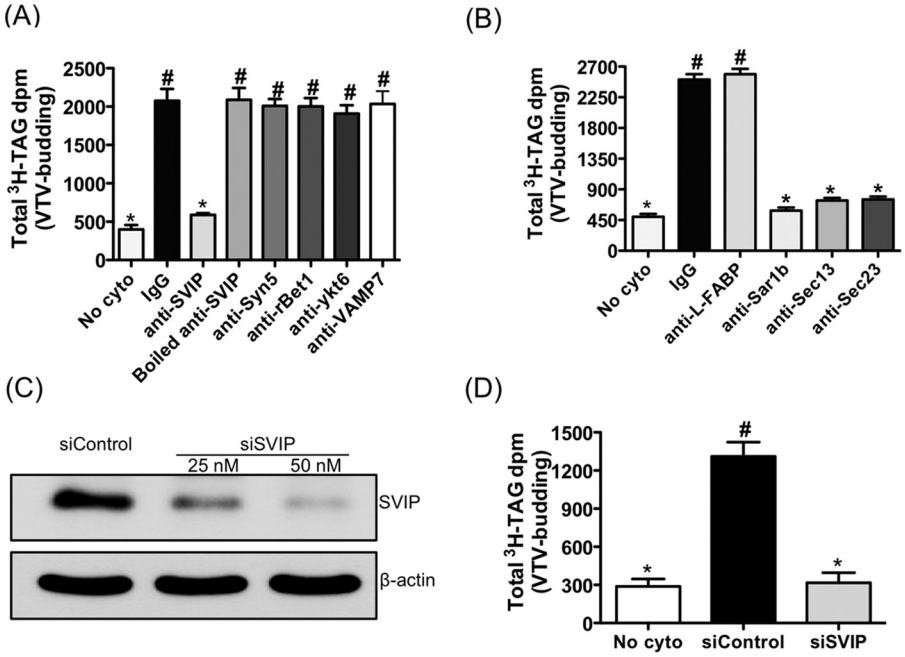

FIGURE 6. **Effects of blocking SVIP and COPII proteins and SVIP knockdown on VTV biogenesis.** *In vitro* VTV formation assays were carried out by incubating hepatic ER containing [^{3}H]TAG with hepatic cytosol and an ATP-regenerating system. After incubation, the reaction mixture was resolved using sucrose continuous density gradient, 0.5-ml fractions were collected, and [^{3}H]TAG dpm in each fraction were determined. *A*, to show the effects of blocking the indicated proteins, ER membranes containing [^{3}H]TAG were incubated at 4 °C for 2 h with preimmune IgG, anti-SVIP, boiled anti-SVIP, anti-syntaxin 5 (*Syn5*), anti-rBet1, anti-ykt6, and anti-VAMP7 antibodies. Postincubation, antibodies in each case were removed by washing. Hepatic cytosol was treated with the indicated antibodies conjugated with agarose beads at 4 °C for 2 h, and antibodies conjugated with agarose beads were pulled down by spinning. As a negative control, VTV formation assay was performed in the absence of cytosol (*No cyto*). *Error bars* depict mean ± S.D. ($n = 4$). *Bars* labeled with different *symbols* demonstrate $p < 0.005$ using one-way ANOVA. *B*, to show the effects of blocking the function of the indicated proteins, ER membranes containing [^{3}H]TAG were incubated at 4 °C for 2 h with preimmune IgG, anti-L-FABP, anti-Sar1b, anti-Sec13, and anti-Sec23 antibodies. Postincubation, antibodies in each case were removed by washing. Hepatic cytosol was treated with the indicated antibodies conjugated with agarose beads at 4 °C for 2 h, and antibodies conjugated with agarose beads were pulled down by spinning. As a negative control, VTV formation assay was performed in the absence of cytosol. *Error bars* represent mean ± S.D. ($n = 4$). *Bars* labeled with different *symbols* demonstrate $p < 0.001$ using one-way ANOVA. *C*, rat hepatocytes were transfected with either two different concentration of SVIP siRNA (25 and 50 nM) or control siRNA (Silencer select siRNA), and whole cell lysates were probed for SVIP and β-actin using specific antibodies. *D*, *in vitro* VTV formation assays were carried out utilizing ER membranes containing [^{3}H]TAG and cytosol that were prepared from hepatocytes transfected with either siSVIP or siControl. As a negative control, the VTV formation assay was performed in the absence of cytosol. *Error bars* represent mean ± S.D. ($n = 4$). *Bars* labeled with different *symbols* depict *p* values using one-way ANOVA: * *versus* #, $p < 0.002$; # *versus* #, *p* is non-significant.

SVIP siRNA-transfected hepatocytes contains either a considerably low level of or no SVIP, whereas the expression of β-actin was unchanged (data not shown).

To demonstrate the effect of SVIP silencing on VTV formation from hepatic ER, we performed an *in vitro* VTV budding assay. Consistent with SVIP blocking data, the process of VTV formation was markedly reduced when SVIP was silenced (Fig. 6*D*). However, VTV generation continued unaffected when cells were treated with control siRNA (Fig. 6*D*). Together, these results strongly demonstrate that SVIP plays a functional role in VTV biogenesis and VLDL exit from the hepatic ER.

Knockdown of SVIP Reduces VLDL Secretion—After confirming an active role of SVIP in the VTV formation process, we sought to determine its effect on overall VLDL secretion from hepatocytes. To achieve this, we knocked down SVIP from primary hepatocytes using SVIP siRNA as described earlier and monitored VLDL secretion by measuring secreted TAG and apoB100 levels in the medium. We incubated SVIP knockdown hepatocytes and control hepatocytes with [^{3}H]oleic acid complexed to BSA at a final concentration of 0.4 mM oleic acid for 1 h. Postincubation, medium containing oleic acid-BSA was removed and replaced with fresh medium without oleic acid-BSA complex. Samples of medium were collected at different time points, and associated [^{3}H]TAG dpm were measured by scintillation counter. The amount of secreted apoB100 was determined by immunoblotting, and the results are summarized in Fig. 7. Because the ER-to-Golgi transport of nascent VLDLs is the rate-limiting factor in their eventual secretion from hepatocytes, we speculated that SVIP silencing would result in reduced VLDL secretion because our data in this report show that SVIP knockdown inhibits VTV formation. As we speculated, secretion of [^{3}H]TAG from SVIP-deficient (knocked down) hepatocytes was significantly reduced as compared with control hepatocytes that were treated with control siRNA (Fig. 7*A*). We observed similar results for apoB100 secretion. The data presented in Fig. 7*B* show that SVIP silencing significantly decreased apoB100 secretion as compared with control (control siRNA). The difference in TAG and apoB100 secretion was maximal at the 24-h time point (Fig. 7, *A* and *B*). Overall, these results strongly suggest that silencing of SVIP reduces VLDL secretion from hepatocytes.

Discussion

Transport of newly synthesized VLDL particles from the hepatic ER to the Golgi plays an important role in their secretion and in controlling overall hepatic lipid metabolism. Once synthesized in the ER lumen, nascent VLDL triggers the formation of a specific ER-derived vesicle, the VTV, for its export to

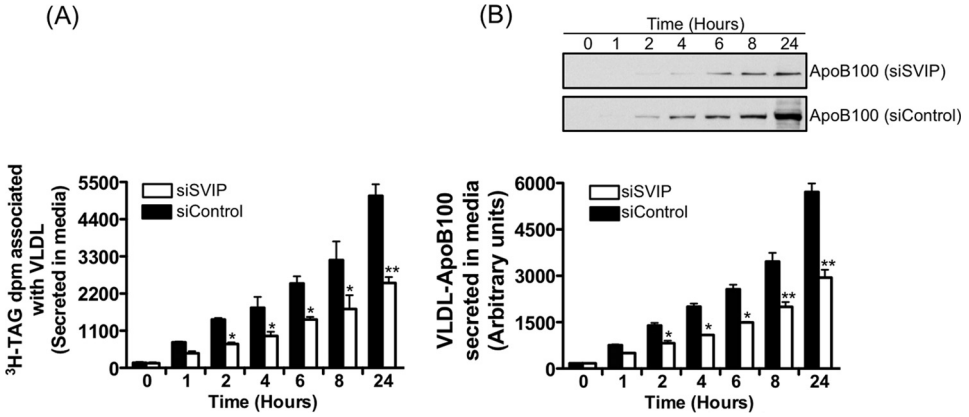

FIGURE 7. **SVIP knockdown reduces TAG and apoB100 secretion.** Rat hepatocytes were transfected with either SVIP siRNA (50 nM) or control siRNA (Silencer select siRNA). *A*, post-transfection, SVIP knockdown hepatocytes and control hepatocytes were washed with warm (37 °C) PBS and incubated with [^{3}H]oleic acid complexed with BSA at a final concentration of 0.4 mM oleic acid for 1 h. Postincubation, medium containing oleic acid-BSA was removed and replaced with fresh medium without oleic acid-BSA complex. Samples of medium were collected at different time points, and associated [^{3}H]TAG dpm were measured by scintillation counter. *Error bars* represent mean ± S.D. ($n = 4$). *Bars* labeled with *asterisks* show *p* values compared with control siRNA using one-way ANOVA: *, $p < 0.01$; **, $p < 0.001$. *B*, for apoB100 secretion by SVIP knockdown and control hepatocytes, medium was collected, and apoB100 was immunoprecipitated using specific anti-apoB100 antibodies. Immunoprecipitated apoB100 was separated by SDS-PAGE and probed by immunoblotting. The amount of secreted apoB100 was determined by analyzing protein band density using the NIH ImageJ program. *Error bars* represent mean ± S.D. ($n = 4$). *Bars* labeled with *asterisks* show *p* values compared with control siRNA using one-way ANOVA: *, $p < 0.01$; **, $p < 0.002$.

the Golgi. Our previous studies have shown that the VTV differs biochemically and morphologically from the classical ER-derived secretory protein transport vesicle and that the genesis of VTV from the ER requires several extra proteins in addition to COPII components (11). A detailed proteomic analysis suggests that a few proteins such as cell death-inducing DFF45-like effector b (cideB), SVIP, LPCAT3, and reticulon 3 are uniquely present in the VTV (10). We have reported earlier that one of these proteins, cideB, is required for the VTV formation from hepatic ER (11). In this study, we characterize a new protein, SVIP, which was originally discovered as an adaptor protein of VCP/p97 and has been implicated in regulating the ERAD and autophagy. SVIP is a very small molecular mass (~9-kDa) cytosolic protein that anchors itself to the cytosolic side of the ER by its N-terminal myristoylation; however, blocking N-terminal myristoylation renders SVIP in cytosol. Here we describe a new physiological role for SVIP in controlling VTV formation from the hepatic ER and VLDL secretion from the hepatocytes.

The exact molecular mechanisms underlying the VLDL selection into VTV and the formation of a larger vesicle (*i.e.* VTV) that can accommodate a VLDL-sized particle remain poorly studied. Originally, it was thought that COPII components are sufficient to select a variety of cargos and able to form a flexible coat-cage, leading to the genesis of a larger vesicle that can accommodate macromolecules; however, an increasing number of studies indicate that COPII coat requires supplementary proteins for both specific cargo selection and large vesicle formation (11, 19, 20). Considering our previous proteomic findings that SVIP is present in VTVs but not in protein transport vesicles or intestinal ER-derived PCTVs, we speculated that SVIP might be playing a role in either VTV biogenesis or VLDL selection into VTVs. Our co-immunoprecipitation studies clearly suggest that SVIP interacts with apoB100 (a VLDL core protein) and Sar1b (a COPII component) at the ER level. Even though SVIP is a peripheral ER protein, its binding with apoB100 is compatible with the membrane topology of ER apoB100, which contains cytosolic domains.

In this study, we have defined a new functional role for SVIP in mediating intracellular VLDL transport between the ER and Golgi. Our data revealed that knockdown of SVIP from the primary rat hepatocytes significantly reduces the VTV biogenesis from the hepatic ER membranes. SVIP has been shown previously to be involved in multiple cellular processes such as the regulation of vacuole formation, autophagy, and inhibition of the ERAD. Of these various functions, formation of large vacuoles is interesting and pertinent to the current investigation because electron microscopic analysis suggests that these vacuoles are derived from the ER. It has been reported that overexpression of SVIP augments vacuole formation from the ER membranes (25). The role of SVIP in intracellular traffic events has not been established; however, it plays an indirect role in lipid-rich prechylomicron trafficking from the intestinal ER to the Golgi. Using a variety of cellular and biochemical techniques, studies from Siddiqi and Mansbach (32) show that SVIP regulates the recruitment of L-FABP on the ER membrane and thus controls the formation of ER-derived prechylomicron transport vesicles. In conjunction with these observations, we claim to have discovered a new functional role of SVIP in VLDL transport and secretion.

The ER membrane generates a number of different types of transport vesicles that carry their distinct cargos to the Golgi, indicating the existence of a robust selection process at the ER level. Consequently, a number of proteins have been identified so far that act in cargo sorting and packaging into specific vesicles. These proteins not only facilitate the selection of their specific cargos into different vesicles, but they also act as adaptors of cargo proteins, allowing interaction with COPII coat proteins and modulating the size of transport vesicles. Recently, 14-3-3, a phosphoregulatory protein, has been shown to act as an adaptor protein for a phosphatidylinositol 4-lipid phosphate, SAC1 (24). SAC1 exits the ER in a COPII-dependent manner; however, its efficient packaging into COPII vesicles requires 14-3-3 protein (24). Utilizing a variety of cell biological and biochemical techniques, it has been shown that the export

of prechylomicrons from the intestinal ER requires four proteins in addition to COPII proteins (20). Kelch-like 12 (KLHL12) protein, which was initially reported to control the Wnt signaling pathway, has been shown to modulate the size of COPII vesicles by ubiquitination of the COPII component Sec31 (33, 34). Ubiquitinated Sec31 yielded larger vesicles that accommodate collagen-sized cargo (33). Interestingly, recent data suggest that ubiquitin ligase KLHL12 also facilitates apoB100 transport and secretion from McARH7777 cells (19). Knockdown of KLHL12 reduces apoB100 secretion, whereas overexpression of this protein enhances the apoB100 secretion (19). In our previous study, we have reported that cideB regulates export of nascent VLDL particles from the ER (11). Others and we have shown that silencing of cideB protein causes reduced VLDL secretion from the primary hepatocytes and that cideB interacts with apoB100 and COPII proteins at the ER level (11, 35). These observations suggest that sorting and packaging of secretory proteins and other cargos into transport carriers are a highly complex process that involves a number of different proteins.

So far three proteins, cideB, KLHL12, and SVIP, have been proposed to facilitate VLDL packaging and formation of larger VLDL-carrying vesicles from the hepatic ER. These findings raise an obvious question. Why does a single cargo (*i.e.* VLDL) need more than one protein for selective packaging into VTVs and exit from the ER? A substantial amount of published data related to the selection of secretory proteins into transport vesicles, which bud off the ER, support the involvement of numerous proteins in cargo selection and vesicle formation (36, 37). Another possibility for such a requirement is that the VLDL particle is considerably large, and its secretion is very important for maintaining overall lipid homeostasis. Hence, to avoid severe consequences of reduced to no VLDL secretion resulting from a single protein malfunction, more than one protein being able to perform the same function (VLDL packaging and VTV formation) could be a part of innate protection mechanism.

Consistent with a specific role in VTV-mediated VLDL export, this study demonstrates a significant reduction in VLDL secretion from hepatocytes that were transfected with SVIP siRNA. This finding is particularly important as it highlights the physiological significance of ER-to-Golgi transport of nascent VLDL particles. Moreover, incubation of primary hepatocytes with myristic acid showed enhanced recruitment of SVIP and Sar1b (budding components of VTV) to the ER membrane, leading to increased VTV formation and thus increased VLDL secretion from the hepatocytes. Because SVIP functions as an inhibitor of ERAD and binds to apoB100 (see "Results"), it is possible that increased SVIP recruitment to the ER protects apoB100 from ERAD. These data are consistent with prior report suggesting that myristic acid induces secretion of lipoproteins by inhibiting apoB100 degradation (39). This study reveals the underlying mechanism of how myristic acid, by facilitating SVIP attachment to the ER and by protecting apoB100, enhances VTV budding and thus VLDL secretion from the hepatocytes.

In summary, we have identified SVIP as a component of the prebudding complex, which is required for the generation of VTV from hepatic ER. Current data revealed a new physiological role of SVIP in the formation of ER-derived VLDL-carrying vesicles and more importantly VLDL secretion from the hepatocytes. Here, we show that the treatment of hepatocytes with myristic acid enhanced the recruitment of VTV budding machinery to the ER membrane and thus provided the molecular mechanism underlying myristic acid-induced lipoprotein secretion. Interaction of SVIP with COPII components and VLDL apoB100 suggested the assembly of an intricate COPII complex that might be necessary for the formation of a larger corral needed for the biogenesis of the VTV-sized vesicle. These findings indicate that different cargos induce the formation of different prebudding complexes for their selection into specific vesicles and that more than one protein in addition to COPII components might be required for effective packaging and generation of a larger transport carrier.

Author Contributions—S. T. and S. S. carried out most of the experiments and analyzed the results. S. S. performed all small animal surgeries to isolate primary hepatocytes. O. Z. performed several experiments to ascertain the reproducibility. S. A. S. conceived and designed the experiments and analyzed the results. S. A. S. and S. T. wrote the paper.

Acknowledgments—We sincerely thank Philip Wessels and Simeon Thibeaux (members of the Siddiqi Laboratory at University of Central Florida, Orlando, FL) for proofreading the manuscript.

References

1. Sundaram, M., and Yao, Z. (2010) Recent progress in understanding protein and lipid factors affecting hepatic VLDL assembly and secretion. *Nutr. Metab.* **7,** 35
2. Sparks, J. D., Sparks, C. E., and Adeli, K. (2012) Selective hepatic insulin resistance, VLDL overproduction, and hypertriglyceridemia. *Arterioscler. Thromb. Vasc. Biol.* **32,** 2104–2112
3. Choi, S. H., and Ginsberg, H. N. (2011) Increased very low density lipoprotein (VLDL) secretion, hepatic steatosis, and insulin resistance. *Trends Endocrinol. Metab.* **22,** 353–363
4. Syed, G. H., Amako, Y., and Siddiqui, A. (2010) Hepatitis C virus hijacks host lipid metabolism. *Trends Endocrinol. Metab.* **21,** 33–40
5. Perlemuter, G., Sabile, A., Letteron, P., Vona, G., Topilco, A., Chrétien, Y., Koike, K., Pessayre, D., Chapman, J., Barba, G., and Bréchot, C. (2002) Hepatitis C virus core protein inhibits microsomal triglyceride transfer protein activity and very low density lipoprotein secretion: a model of viral-related steatosis. *FASEB J.* **16,** 185–194
6. Mirandola, S., Bowman, D., Hussain, M. M., and Alberti, A. (2010) Hepatic steatosis in hepatitis C is a storage disease due to HCV interaction with microsomal triglyceride transfer protein (MTP). *Nutr. Metab.* **7,** 13
7. Tiwari, S., and Siddiqi, S. A. (2012) Intracellular trafficking and secretion of VLDL. *Arterioscler. Thromb. Vasc. Biol.* **32,** 1079–1086
8. Siddiqi, S. A. (2008) VLDL exits from the endoplasmic reticulum in a specialized vesicle, the VLDL transport vesicle, in rat primary hepatocytes. *Biochem. J.* **413,** 333–342
9. Gusarova, V., Brodsky, J. L., and Fisher, E. A. (2003) Apolipoprotein B100 exit from the endoplasmic reticulum (ER) is COPII-dependent, and its lipidation to very low density lipoprotein occurs post-ER. *J. Biol. Chem.* **278,** 48051–48058
10. Rahim, A., Nafi-valencia, E., Siddiqi, S., Basha, R., Runyon, C. C., and Siddiqi, S. A. (2012) Proteomic analysis of the very low density lipoprotein (VLDL) transport vesicles. *J. Proteomics* **75,** 2225–2235
11. Tiwari, S., Siddiqi, S., and Siddiqi, S. A. (2013) CideB protein is required for the biogenesis of very low density lipoprotein (VLDL) transport vesicle. *J. Biol. Chem.* **288,** 5157–5165
12. Siddiqi, S., Mani, A. M., and Siddiqi, S. A. (2010) The identification of the

SNARE complex required for the fusion of VLDL-transport vesicle with hepatic cis-Golgi. *Biochem. J.* **429,** 391–401
13. Gusarova, V., Seo, J., Sullivan, M. L., Watkins, S. C., Brodsky, J. L., and Fisher, E. A. (2007) Golgi-associated maturation of very low density lipoproteins involves conformational changes in apolipoprotein B, but is not dependent on apolipoprotein E. *J. Biol. Chem.* **282,** 19453–19462
14. Tran, K., Thorne-Tjomsland, G., DeLong, C. J., Cui, Z., Shan, J., Burton, L., Jamieson, J. C., and Yao, Z. (2002) Intracellular assembly of very low density lipoproteins containing apolipoprotein B100 in rat hepatoma McA-RH7777 cells. *J. Biol. Chem.* **277,** 31187–31200
15. Barlowe, C., Orci, L., Yeung, T., Hosobuchi, M., Hamamoto, S., Salama, N., Rexach, M. F., Ravazzola, M., Amherdt, M., and Schekman, R. (1994) COPII: a membrane coat formed by Sec proteins that drive vesicle budding from the endoplasmic reticulum. *Cell* **77,** 895–907
16. D'Arcangelo, J. G., Stahmer, K. R., and Miller, E. A. (2013) Vesicle-mediated export from the ER: COPII coat function and regulation. *Biochim. Biophys. Acta* **1833,** 2464–2472
17. Miller, E. A., and Barlowe, C. (2010) Regulation of coat assembly—sorting things out at the ER. *Curr. Opin. Cell Biol.* **22,** 447–453
18. Gillon, A. D., Latham, C. F., and Miller, E. A. (2012) Vesicle-mediated ER export of proteins and lipids. *Biochim. Biophys. Acta* **1821,** 1040–1049
19. Butkinaree, C., Guo, L., Ramkhelawon, B., Wanschel, A., Brodsky, J. L., Moore, K. J., and Fisher, E. A. (2014) A regulator of secretory vesicle size, Kelch-like protein 12, facilitates the secretion of apolipoprotein B100 and very-low-density lipoproteins—brief report. *Arterioscler. Thromb. Vasc. Biol.* **34,** 251–254
20. Siddiqi, S., Saleem, U., Abumrad, N. A., Davidson, N. O., Storch, J., Siddiqi, S. A., and Mansbach, C. M., 2nd (2010) A novel multiprotein complex is required to generate the prechylomicron transport vesicle from intestinal ER. *J. Lipid Res.* **51,** 1918–1928
21. Neeli, I., Siddiqi, S. A., Siddiqi, S., Mahan, J., Lagakos, W. S., Binas, B., Gheyi, T., Storch, J., and Mansbach, C. M., 2nd (2007) Liver fatty acid-binding protein initiates budding of pre-chylomicron transport vesicles from intestinal endoplasmic reticulum. *J. Biol. Chem.* **282,** 17974–17984
22. Mansbach, C. M., and Siddiqi, S. A. (2010) The biogenesis of chylomicrons. *Annu. Rev. Physiol.* **72,** 315–333
23. Miller, E. A., and Schekman, R. (2013) COPII—a flexible vesicle formation system. *Curr. Opin. Cell Biol.* **25,** 420–427
24. Bajaj Pahuja, K., Wang, J., Blagoveshchenskaya, A., Lim, L., Madhusudhan, M. S., Mayinger, P., and Schekman, R. (2015) Phosphoregulatory protein 14-3-3 facilitates SAC1 transport from the endoplasmic reticulum. *Proc. Natl. Acad. Sci. U.S.A.* **112,** E3199–E3206
25. Nagahama, M., Suzuki, M., Hamada, Y., Hatsuzawa, K., Tani, K., Yamamoto, A., and Tagaya, M. (2003) SVIP is a novel VCP/p97-interacting protein whose expression causes cell vacuolation. *Mol. Biol. Cell* **14,** 262–273
26. Ballar, P., Zhong, Y., Nagahama, M., Tagaya, M., Shen, Y., and Fang, S. (2007) Identification of SVIP as an endogenous inhibitor of endoplasmic reticulum-associated degradation. *J. Biol. Chem.* **282,** 33908–33914
27. Liang, J. S., Kim, T., Fang, S., Yamaguchi, J., Weissman, A. M., Fisher, E. A., and Ginsberg, H. N. (2003) Overexpression of the tumor autocrine motility factor receptor Gp78, a ubiquitin protein ligase, results in increased ubiquitinylation and decreased secretion of apolipoprotein B100 in HepG2 cells. *J. Biol. Chem.* **278,** 23984–23988
28. Olofsson, S. O., and Borèn, J. (2005) Apolipoprotein B: a clinically important apolipoprotein which assembles atherogenic lipoproteins and promotes the development of atherosclerosis. *J. Intern. Med.* **258,** 395–410
29. Siddiqi, S. A., Siddiqi, S., Mahan, J., Peggs, K., Gorelick, F. S., and Mansbach, C. M., 2nd (2006) The identification of a novel endoplasmic reticulum to Golgi SNARE complex used by the prechylomicron transport vesicle. *J. Biol. Chem.* **281,** 20974–20982
30. Siddiqi, S. A. (2015) *In vitro* analysis of the very-low density lipoprotein export from the trans-Golgi network. *Curr. Protoc. Cell Biol.* **67,** 11.21.1–11.21.17
31. Hossain, T., Riad, A., Siddiqi, S., Parthasarathy, S., and Siddiqi, S. A. (2014) Mature VLDL triggers the biogenesis of a distinct vesicle from the trans-Golgi network for its export to the plasma membrane. *Biochem. J.* **459,** 47–58
32. Siddiqi, S., and Mansbach, C. M., 2nd (2012) Phosphorylation of Sar1b protein releases liver fatty acid-binding protein from multiprotein complex in intestinal cytosol enabling it to bind to endoplasmic reticulum (ER) and bud the pre-chylomicron transport vesicle. *J. Biol. Chem.* **287,** 10178–10188
33. Jin, L., Pahuja, K. B., Wickliffe, K. E., Gorur, A., Baumgärtel, C., Schekman, R., and Rape, M. (2012) Ubiquitin-dependent regulation of COPII coat size and function. *Nature* **482,** 495–500
34. Angers, S., Thorpe, C. J., Biechele, T. L., Goldenberg, S. J., Zheng, N., MacCoss, M. J., and Moon, R. T. (2006) The KLHL12-Cullin-3 ubiquitin ligase negatively regulates the Wnt-β-catenin pathway by targeting Dishevelled for degradation. *Nat. Cell Biol.* **8,** 348–357
35. Ye, J., Li, J. Z., Liu, Y., Li, X., Yang, T., Ma, X., Li, Q., Yao, Z., and Li, P. (2009) Cideb, an ER- and lipid droplet-associated protein, mediates VLDL lipidation and maturation by interacting with apolipoprotein B. *Cell Metab.* **9,** 177–190
36. Powers, J., and Barlowe, C. (2002) Erv14p directs a transmembrane secretory protein into COPII-coated transport vesicles. *Mol. Biol. Cell* **13,** 880–891
37. Barlowe, C. (1998) COPII and selective export from the endoplasmic reticulum. *Biochim. Biophys. Acta* **1404,** 67–76
38. Shrivastav, A., Pasha, M. K., Selvakumar, P., Gowda, S., Olson, D. J., Ross, A. R., Dimmock, J. R., Sharma, R. K. (2003) Potent inhibitor of N-myristoylation: a novel molecular target for cancer. *Cancer Res.* **63,** 7975–7978
39. Kummrow, E., Hussain, M. M., Pan, M., Marsh, J. B., and Fisher, E. A. (2002) Myristic acid increases dense lipoprotein secretion by inhibiting apoB degradation and triglyceride recruitment. *J. Lipid Res.* **43,** 2155–2163
40. Siddiqi, S. A., Gorelick, F. S., Mahan, J. T., and Mansbach, C. M., 2nd (2003) COPII proteins are required for Golgi fusion but not for endoplasmic reticulum budding of the pre-chylomicron transport vesicle. *J. Cell Sci.* **116,** 415–427